

Stable Bosonic Topological Edge Modes in the Presence of Many-Body Interactions

Niclas Heinsdorf,^{1,2} Darshan G. Joshi,³ Hosho Katsura,^{4,5,6} and Andreas P. Schnyder¹

¹*Max-Planck-Institut für Festkörperforschung, Heisenbergstrasse 1, D-70569 Stuttgart, Germany*

²*Department of Physics and Astronomy & Stewart Blusson Quantum Matter Institute, University of British Columbia, Vancouver BC, Canada V6T 1Z4*

³*Tata Institute of Fundamental Research, Hyderabad 500046, India*

⁴*Department of Physics, Graduate School of Science, The University of Tokyo, 7-3-1 Hongo, Tokyo 113-0033, Japan*

⁵*Institute for Physics of Intelligence, The University of Tokyo, 7-3-1 Hongo, Tokyo 113-0033, Japan*

⁶*Trans-scale Quantum Science Institute, The University of Tokyo, 7-3-1, Hongo, Tokyo 113-0033, Japan*

(Dated: September 27, 2023)

Many magnetic materials are predicted to exhibit bosonic topological edge modes in their excitation spectra, because of the nontrivial topology of their magnon, triplon or other quasi-particle band structures. However, there is a discrepancy between theory prediction and experimental observation, which suggests some underlying mechanism that intrinsically suppresses the expected experimental signatures, like the thermal Hall current. Many-body interactions that are not accounted for in the non-interacting quasi-particle picture are most often identified as the reason for the absence of the topological edge modes. Here we report stable bosonic edge modes at the boundaries of a ladder quantum paramagnet with gapped triplon excitations in the presence of the full many-body interaction. For the first time, we use tensor network methods to resolve topological edge modes in the time-dependent spin-spin correlations and the dynamical structure factor, which is directly accessible experimentally. We further show that these edge modes have anomalously long time coherence, discuss the topological phase diagram of the model, demonstrate the fractionalization of its low-lying excitations, and propose potential material candidates.

The enormous success of the description of electronic topological phases of matter quickly inspired research that lead to the generalization of the theory to bosonic quasi-particles like photons [1–6], phonons [7–10], magnons [11–19] or triplons [20–22]. Analogous to the Quantum or Spin Hall effect for electrons, the non-trivial topology of magnetic excitations contributes to unusual responses like the Thermal Hall or Spin Nernst effect in the form of bosonic edge currents.

These topologically protected edge spin waves are a key ingredient for many future spintronic applications, which are a promising alternative to conventional computing, but with a minimal ecological footprint[23]. There is a multitude of blueprints that make use of their properties to build next-generation devices like spin-wave diodes, beam splitters, interferometers and others [23–26].

Moreover, systems that are useful for storing and processing quantum information are highly sought-after. Typically, the quantum information of a many-body state is destroyed rapidly. Overcoming fast decoherence of quantum states is one of the main challenges of quantum computing, and has driven extensive theoretical interest in finding ways to increase their coherence times using many-body localization [27–31], prethermalization [32–34], quantum many-body scarring [35–37] or the states' topological properties[38–41]. The evolution of topological states over time - specifically in the presence of defects or nonlinearities[42–44] - as well as imaging and detection techniques[45–47] are thriving fields of research and crucial for bringing real-world applications on their way.

Even though a significant amount of material candidates has been proposed to host nontrivial excita-

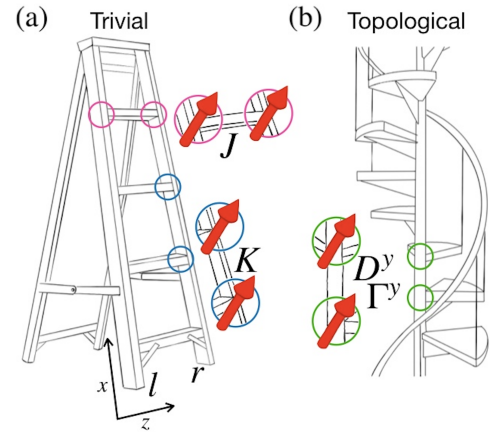


FIG. 1. (a) Schematic of the spin model on a ladder geometry. On each rung of the ladder, two spin-1/2 sites are (strongly) coupled through antiferromagnetic Heisenberg interaction. Along the side rails, the spins interact (weakly) antiferromagnetically. In this limit the spins form singlet pairs along the rungs of the ladder. (b) The same model but with anti-symmetric (DM) and symmetric (pseudo-dipolar) exchange in the y -direction given by D_y and Γ_y . These terms introduce a winding and open a topological gap in the excitation spectrum.

tions [11, 14, 20, 25, 48–54], their detection remains elusive. While some experiments indeed show signatures of the predicted bosonic edge modes[55–60], others have not been able to produce evidence of topological quasi-particles [61, 62], and for most of the proposed candidates a clear indication of their presence is yet to be discovered.

Many reasons that could make the effects of the topological edge modes fail to materialize have been theorized. Among other things, they include thermal dampening, magnon-phonon coupling and domain formation, but what is most often identified as the source of the suppression of thermal Hall effect are many-body effects. In contrast to their fermionic counterparts, even small many-body interactions [61, 63, 64] or exchange anisotropies that are typically present in realistic models [65] seem to substantially affect bosonic topological transport properties.

In this work we report bosonic topological edge modes that are stable in the presence of the full many-body interaction using Density Matrix Renormalization Group (DMRG) and time-evolution methods.

Model and Harmonic Approximation.—We consider a quantum $S = 1/2$ Heisenberg model on a ladder with spin-orbit interaction and an external magnetic field as shown schematically in Fig. 1. This model, first considered in Ref. [21] is given by the following Hamiltonian:

$$\hat{H} = \hat{H}_{\text{rung}} + \hat{H}_{\text{rail}} + \hat{H}_{\text{SOC}} + \hat{H}_Z, \quad (1)$$

$$\hat{H}_{\text{rung}} = J \sum_i \hat{S}_{li} \cdot \hat{S}_{ri}, \quad (2)$$

$$\hat{H}_{\text{rail}} = K \sum_i \left(\hat{S}_{li} \cdot \hat{S}_{li+1} + \hat{S}_{ri} \cdot \hat{S}_{ri+1} \right), \quad (3)$$

$$\begin{aligned} \hat{H}_{\text{SOC}} = D_y \sum_{\alpha=l,r} \sum_i \left(\hat{S}_{\alpha i}^z \hat{S}_{\alpha i+1}^x - \hat{S}_{\alpha i}^x \hat{S}_{\alpha i+1}^z \right), \\ + \Gamma_y \sum_{\alpha=l,r} \sum_i \left(\hat{S}_{\alpha i}^z \hat{S}_{\alpha i+1}^x + \hat{S}_{\alpha i}^x \hat{S}_{\alpha i+1}^z \right), \end{aligned} \quad (4)$$

$$\hat{H}_Z = h_y \sum_{\alpha=l,r} \sum_i \left(\hat{S}_{\alpha i}^y + \hat{S}_{\alpha i}^y \right), \quad (5)$$

where $\hat{S}_{\alpha i} = \left(\hat{S}_{\alpha i}^x, \hat{S}_{\alpha i}^y, \hat{S}_{\alpha i}^z \right)^T$ are the usual spin operators with $\alpha = l, r$ corresponding to the left and right rail of the ladder and i running over all rungs at positions r_i .

In the limit of strong anti-ferromagnetic rung coupling, this model is the prototypical example of a gapped quantum paramagnet [66, 67]. In that limit the ground state of the model is close to a product state of spin singlets

$$|\psi_0\rangle \sim \bigotimes_{i=1}^L (|\uparrow\downarrow\rangle - |\downarrow\uparrow\rangle) / \sqrt{2}, \quad (6)$$

with low-lying triplet excitations, the corresponding quasiparticles being triplons. In the presence of SU(2) symmetry ($D_y = \Gamma_y = h_y = 0$), the triplons are degenerate, but can be split by applying an external magnetic field due to their different magnetic quantum number. Alternatively, the degeneracy can be lifted through spin-orbit interactions. Its anti-symmetric part - similar to the magnetic field term - splits the triplon modes while retaining U(1) symmetry. The pseudo-dipolar, or Γ -term, which is the symmetric part of the spin-orbit interaction breaks U(1)-symmetry.

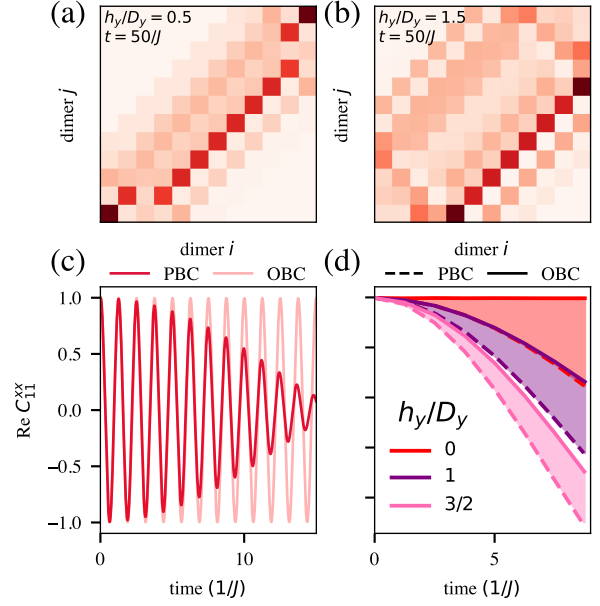


FIG. 2. Real part of the spin-spin correlation function at time $t = 50/J$ in the (a) trivial and (b) the topological case with $K = 0.01J$ and field strengths $h_y/D_y = 0.5$ and $h_y/D_y = 1.5$ respectively on a ladder with $L = 12$ rungs. The topological auto-correlation at this time step has peaks at the boundaries, which are absent in the trivial case. (c) Time dependence of the boundary auto-correlation $\text{Re } C_{11}^{zz}$ for $K = 0.01J$, $D_y = \Gamma_y = 0.1J$ and no magnetic field on a ladder with $L = 8$ rungs for different boundary conditions. For PBC (no in-gap mode), it decays rapidly whereas for OBC (in-gap mode) it does not decay. (d) The decay envelopes of (c) for different values of magnetic field. For finite field strengths the correlator decays also for OBC, but more slowly than for PBC.

In the paramagnetic phase of the model, an effective low-energy spectrum can be calculated by first rewriting the model in terms of triplons through bond-operator theory[68], and then discarding all resulting terms that are not bilinear, which has been shown to be a controlled approximation [69, 70]. Within this harmonic approximation, it was shown in Ref. [21] that the so-obtained excitation spectrum can be characterized by a topological winding number that classifies the topology of the magnet's bulk and enforces - if nontrivial - triplon modes at the ends of the ladder with fractional particle number.

In contrast to the case of topological magnons of ordered magnets [59, 71–75] - where there is a gapless Goldstone mode - the triplon excitations in the quantum paramagnet are gapped. As a consequence of this bulk gap the triplons, including the topological edge modes, do not have any low-energy states to decay into. Therefore their lifetime is not reduced significantly even in the presence of interactions. By applying an external magnetic field or through spin-anisotropy exchanges, magnon systems can become gapless too. However, a bulk gap induced by these effects is typically much smaller than the rung

coupling J , which is the relevant spin exchange energy scale that determines the size of the gap in the ladder system.

The spin model presented herein is suitable to describe the magnetism of potentially many materials and belongs to the well studied class of two-leg ladder compounds. Examples of spin ladder materials are BiCu_2PO_6 [76], NaV_2O_5 [77, 78] or multiple cuprate ladders[79–82]. The recipe for finding topological edge modes in these systems requires mainly two ingredients: (i) strong anti-ferromagnetic rung coupling (stronger than along the rails), and (ii) spin-orbit interaction. Because the Heisenberg couplings along the rungs and rails depend on the overlap of the localized electrons, their ratio can easily be tuned using e.g. strain. The same is true for the relative spin-orbit interaction strength[83–86], however, the D and Γ term are additionally restricted by symmetries. These symmetries can be broken, if not already broken internally, by doping, gate voltages or structural manipulations like skewing and stretching. The abundance of experimental handles suggests that a topological phase transition might easily be switchable, which again expands the potential applications of these systems in future devices.

Tensor Networks and Dynamical Response.—To relate our model directly to an experimentally measurable quantity, we compute the dynamic structure factor (DSF), which is most directly accessed through inelastic neutron scattering[87, 88] or inverse spin Hall noise spectroscopy (ISHNS)[89]. Because we are investigating the effect of interactions, and since our model is (quasi) one-dimensional, we use the DRMG algorithm to obtain the exact many-body ground state of the finite spin ladder[90].

In contrast to electronic systems, the band topology of bosonic quasiparticles is not a ground state property, so in order to access the low-lying excitations, we apply time-evolution methods[91–96] to compute the odd-part of the time-dependent spin-spin correlation

$$C_{ij}^{\gamma\gamma'}(t) = \langle \psi_0 | \hat{S}_i^\gamma \hat{U}(t) \hat{S}_j^{\gamma'} | \psi_0 \rangle, \quad (7)$$

with $\hat{S}_i^\gamma = \hat{S}_{i_i}^\gamma - \hat{S}_{r_i}^\gamma$ and the unitary time-evolution operator $\hat{U}(t)$. Already the real-space and -time correlation function shows signatures of edge modes in the topologically nontrivial phase region ($h_y < |D|$). In Fig. 2 (a) and (b) the real part of $C_{ij}^{\gamma\gamma'}(t)$ for the topological and trivial case at a fixed time step are plotted. The former shows strong correlations that are pinned to the edges of the system, whereas they are absent in the latter.

In Fig. 2 (c), we plot the time dependence of $\text{Re } C_{11}^{xx}$ at zero magnetic field for periodic (PBC) and open boundary conditions (OBC). For PBC there is no topologically protected edge mode at $i = j = 1$, and the excitation decays over time rapidly. In the open system the edge mode has strongly enhanced time coherence, and we cannot resolve any decay during the time it takes the excitation to hit the boundary at the other end of the ladder. Fig. 2 (d)

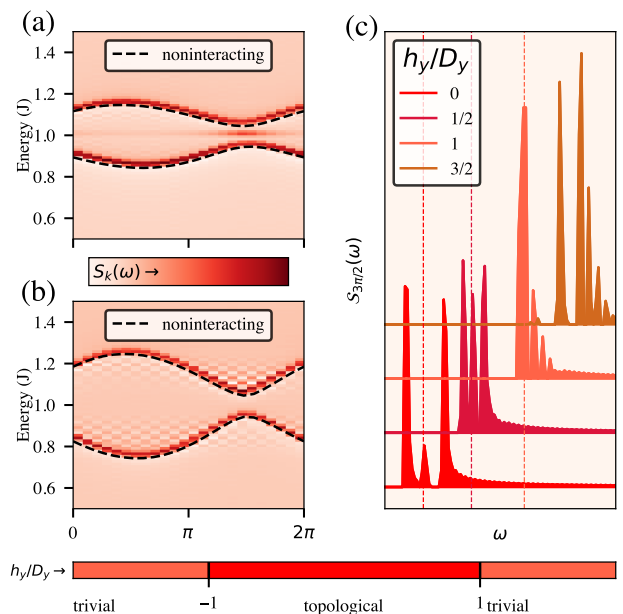


FIG. 3. $S_k(\omega)$ for the (a) topological and (b) trivial quantum paramagnet with $h_y/D_y = 1/2$ and $h_y/D_y = 3/2$ respectively on a ladder with $L = 12$ rungs. The dashed line shows the spectrum of the effective low-energy models from Ref. [21]. (c) $S_{3\pi/2}(\omega)$ for different values of h_y/D_y . The first two curves lie in the topological phase region (see phase diagram at the bottom) with the in-gap modes marked by dashed lines. At $h_y/D_y = 1$ the gap is closed. The last curve lies in the trivial region and is gapped, with no mode in-between.

shows the decay envelope of the excitation for increasing magnetic field for periodic (dashed line) and open (solid line) boundaries. For finite magnetic fields the boundary correlation starts to decay, and for stronger fields the difference in lifetime for PBC and OBC - as indicated by the shaded area - becomes less pronounced.

The DSF, which encodes the dynamical susceptibility of the paramagnet is defined as the Fourier transform of the spin-spin correlations in space and time

$$S_k^{\gamma\gamma'}(\omega) = \frac{1}{2\pi L} \int_{-\infty}^{\infty} dt e^{i(\omega - \omega_0)t} \sum_{i,j} e^{i(r_j - r_i)k} C_{ij}^{\gamma\gamma'}(t). \quad (8)$$

It is a positive and real quantity and can be calculated using DMRG and time-evolution methods. Usually, the system size and parameters of the time-evolution are chosen to minimize finite size effects, and the state is evolved only for as long as the excitation does not reach the boundary of the system. In addition, by imposing translational invariance, one of the spatial degrees of freedom of $C_{ij}^{\gamma\gamma'}(t)$ can be fixed [97–100]. Because we are explicitly studying the excitations in the presence of a boundary, we require the “full” real-space correlation function, as well as a “long-enough” time-evolution. $S_k^{\gamma\gamma'}(\omega)$ obeys sum rules[99] that we track to diagnose the severity of

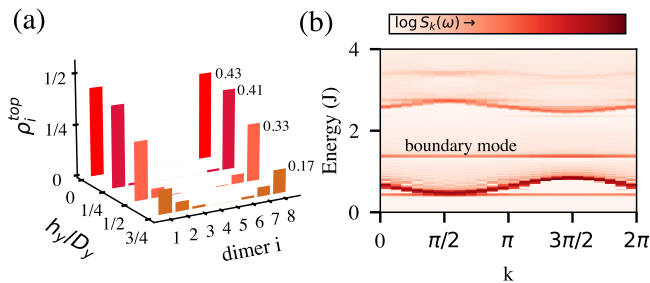


FIG. 4. (a) Topological density of states ρ_i^{top} for $K = 0.01J$, $D_y = \Gamma_y = 0.1J$ and different values of h_y on a ladder with $L = 8$ rungs. The in-gap mode is localized at the two boundaries of the system with fractional particle numbers at each termination. For finite magnetic field the in-gap mode spreads into the bulk and vanishes at the topological phase transition at $h_y/D_y = 1$. (b) The logarithm of the DSF for $K = 0.01J$, $h_y = 0.2$ and strong SOC $D_y = \Gamma_y = 1.2J$ on a ladder with $L = 12$ rungs. The quasi-particle peaks are dampened and split. The boundary mode is flat and marked by text.

finite-time and -size effects, which lead to numerical artifacts (see supplementary material[101]).

We study the field-susceptible part of Eq. (8) which is given by $S_k(\omega) = S_k^{xx}(\omega) + S_k^{zz}(\omega)$ to which we simply refer to as DSF from now.

Results.—In Fig. 3 (a) and (b) we plot the DSF of the topological and trivial paramagnet along with the triplon bands obtained within the harmonic approximation in Ref. [21]. For small rail and spin-orbit coupling the harmonic approximation is accurate, because the density of triplons is small leading to only minor renormalizations from triplon-triplon interactions. In the topologically nontrivial case (small values of magnetic field) an additional mode appears between the two bulk bands that we hereafter refer to as *in-gap mode*. It is absent in the trivial phase (large values of magnetic field). Fig. 3 (c) shows the topological phase transition at $k = 3\pi/2$ with the external magnetic field h_y as a tuning parameter. At $h_y = |D_y|$ the gap closes, and further increasing the magnetic field it reopens, but with no topological in-gap mode. We did finite size scaling with ladders of up to $L = 24$ rungs to confirm that the in-gap mode retains finite spectral weight.

To confirm that the in-gap mode is really localized at the boundaries of the system, we first calculate the local density of states of the lower band

$$\rho_i = \sum_k e^{-ir_j k} \int_0^{J+\delta} d\omega S_k(\omega), \quad (9)$$

where δ is a small enough value such that the spectral weight of any boundary mode, but not that of the upper triplon band is included in the integral. We then define the “topological density of states” as the difference of the local densities of states of the nontrivial paramagnet for

open and periodic boundary conditions [21]

$$\rho_i^{\text{top}} = \rho_i^{\text{OBC}} - \rho_i^{\text{PBC}}. \quad (10)$$

This quantity isolates the contribution to the spectrum that stems from introducing a boundary and is shown Fig. 4 (a) for different values of magnetic field. We see two peaks located at the boundary of the ladder, that start to spread into the bulk for finite fields. To compute the associated particle number at one of the edges we integrate ρ_i^{top} for the system’s left termination

$$n_t = \int_1^{L/2} dr \rho_i^{\text{top}}, \quad (11)$$

and find that the edge mode has fractional particle number. Our numerical result $n_t \sim 0.43$ deviates slightly from the predicted value of 0.5 [21] due to spectral leakage caused by the aforementioned finite-size and time effects. However we expect that in the thermodynamic limit this value would indeed tend to 0.5. For larger values of field n_t becomes smaller and vanishes at the phase transition at $h_y/D_y = 1$.

The noninteracting triplon winding number is a topological band property[21], so the edge modes are naively expected to be stable only as long as there is a notion of “bands”, or in other words as long as triplons provide a suitable quasi-particle description of the ladder’s excitation spectrum. We consider three limits of the model’s parameter space: (i) large magnetic field h_y , (ii) large rail coupling K and (iii) large spin-orbit interaction D_y and Γ_y . In case (i), the field-polarized phase, the lower triplon modes condenses at $h_y \sim J$ and the system becomes ferromagnetic with magnons as its low-lying excitations. The band structures derived from linear spin wave theory are given in the supplementary material[101] and are topologically trivial. Case (ii) is the limit of two weakly coupled anti-ferromagnetic Heisenberg chains. The system does not order, even for strong rail coupling ($K \sim 2J$). The antiferromagnetic order parameter is finite also for small values of K , but approaches zero as the system size L is increased, as confirmed by finite size scaling [101]. Case (iii) is the most relevant benchmark of the edge modes’ stability that we can provide with the available handles in the model, because here the higher-order terms of the interacting triplon Hamiltonian become important[21]. In this limit there is significant overlap with the two- and three-triplon continuum that leads to damping and decay, and the quasi-particle description within the harmonic approximation breaks down. In contrast to case (i), increasing of D_y and Γ_y does not lead to condensation of the lower mode, and we did not find any evidence for a phase transition up to values of $D_y = \Gamma_y = 2.6J$. In Fig. 4 (b) we plot the logarithm of the DSF for $D_y = \Gamma_y = 1.2J$. Even though the upper triplon band is strongly damped and split into many energy levels, we find that the topological edge modes remain stable.

Conclusion—We have demonstrated that, contrary to what the absence of experimental evidence for many predicted materials might suggest, topological bosonic edge modes can be stable in the presence of the full many-body interaction. Even though correlations have been identified as the reason for the absence of topological responses in some cases, our work clearly shows that they do not generically suppress bosonic edge modes, and it prompts the question of what other mechanism is responsible. A natural extension of this work is to apply our method to two-dimensional systems wrapped onto a cylinder. Multi-rail ladders[102, 103], a ferromagnet on a Lieb lattice[104] or the Shastry-Sutherland model[105] are obvious candidates, but also topological magnon systems that are potentially more fragile due to their larger decay phase space.

The absence of signatures of topological edge modes even in systems with good agreement between theory and experiment for bulk properties suggests that the responsible decay channel might be a surface effect, i.e., it lies at the boundary. In a quasi two-dimensional model the edge modes are not completely localized, but propagate along the boundary of the system. This setup would further allow the implementation of a defect at the boundary and to investigate the stability of the topological bosons in its presence.

The typical “workflow” for finding topological edge modes usually consists of classifying the topology of a translationally invariant model, and then inferring their existence by bulk-boundary correspondence. Even if the symmetry that protects the band topology is broken weakly, the edge states are still expected to be present as long as the the perturbation is smaller than the gap they live in (these approximate symmetries are sometimes called quasi-symmetries[106, 107]). The chiral symme-

try that allows for the definition of a winding number in the noninteracting case is broken by the rail coupling K [21], and is also clearly broken in the limit of strong SOC, nevertheless our numerical study shows that the edge modes persist, which invokes the question of a more suitable bulk classification.

In recent years, considerable effort has been invested in the extension of topological classifications to interacting systems [108–113]. These schemes account for the many-body nature of the problem using either a matrix product state or Green’s function representation, but are not applicable for the classification of bosonic excitation spectra. Detection of phase transitions using entanglement have been brought forward, but are - even though directly related to the dynamical response of a spin system - not sensitive to topological phase transitions[114]. It is essential to extend existing or find new methods that are able to capture the topological properties of e.g. dynamical spin responses, and we hope our work inspires fruitful research in that direction.

ACKNOWLEDGMENTS

We thank A. Nocera and S. M. Winter for helpful discussions. NH acknowledges financial support from the Max Planck Institute for Solid State Research in Stuttgart, Germany and the DAAD JSPS summer program 2022. DGJ acknowledges support from the Department of Atomic Energy, Government of India, under Project Identification No. RTI 4007. A.P.S. and N.H. acknowledge support by the Deutsche Forschungsgemeinschaft (DFG, German Research Foundation) – TRR 360 – 492547816. H.K. was supported by JSPS KAKENHI Grant No. JP23H01093 and MEXT KAKENHI Grant-in-Aid for Transformative Research Areas A “Extreme Universe” (KAKENHI Grant No. JP21H05191).

-
- [1] Onur Hosten and Paul Kwiat. Observation of the spin hall effect of light via weak measurements. *Science*, 319(5864):787–790, 2008.
 - [2] Zheng Wang, Yidong Chong, John D Joannopoulos, and Marin Soljačić. Observation of unidirectional backscattering-immune topological electromagnetic states. *Nature*, 461(7265):772–775, 2009.
 - [3] Philippe Ben-Abdallah. Photon thermal hall effect. *Physical Review Letters*, 116(8):084301, 2016.
 - [4] Frederick Duncan Michael Haldane and Srinivas Raghu. Possible realization of directional optical waveguides in photonic crystals with broken time-reversal symmetry. *Physical Review Letters*, 100(1):013904, 2008.
 - [5] Srinivas Raghu and Frederick Duncan Michael Haldane. Analogs of quantum-hall-effect edge states in photonic crystals. *Physical Review A*, 78(3):033834, 2008.
 - [6] Masaru Onoda, Shuichi Murakami, and Naoto Nagaosa. Hall effect of light. *Physical review letters*, 93(8):083901, 2004.
 - [7] C Strohm, GLJA Rikken, and P Wyder. Phenomenological evidence for the phonon hall effect. *Physical Review Letters*, 95(15):155901, 2005.
 - [8] Yu Kagan and LA Maksimov. Anomalous hall effect for the phonon heat conductivity in paramagnetic dielectrics. *Physical Review Letters*, 100(14):145902, 2008.
 - [9] Kaori Sugii, Masaaki Shimozawa, Daiki Watanabe, Yoshitaka Suzuki, Mario Halim, Motoi Kimata, Yosuke Matsumoto, Satoru Nakatsuji, and Minoru Yamashita. Thermal hall effect in a phonon-glass ba 3 cusb 2 o 9. *Physical Review Letters*, 118(14):145902, 2017.
 - [10] L Sheng, DN Sheng, and CS Ting. Theory of the phonon hall effect in paramagnetic dielectrics. *Physical Review Letters*, 96(15):155901, 2006.
 - [11] Hoshio Katsura, Naoto Nagaosa, and Patrick A. Lee. Theory of the thermal hall effect in quantum magnets. *Phys. Rev. Lett.*, 104:066403, Feb 2010.
 - [12] Hiroki Kondo, Yutaka Akagi, and Hoshio Katsura. Three-dimensional topological magnon systems. *Physical Review B*, 100(14):144401, 2019.
 - [13] Hiroki Kondo and Yutaka Akagi. Dirac surface states in magnonic analogs of topological crystalline insulators.

- Physical Review Letters, 127(17):177201, 2021.
- [14] Ryo Matsumoto and Shuichi Murakami. Rotational motion of magnons and the thermal hall effect. *Physical Review B*, 84(18):184406, 2011.
- [15] Satoshi Fujimoto. Hall effect of spin waves in frustrated magnets. *Physical Review Letters*, 103(4):047203, 2009.
- [16] Ryuichi Shindou, Jun-ichiro Ohe, Ryo Matsumoto, Shuichi Murakami, and Eiji Saitoh. Chiral spin-wave edge modes in dipolar magnetic thin films. *Physical Review B*, 87(17):174402, 2013.
- [17] Ryuichi Shindou, Ryo Matsumoto, Shuichi Murakami, and Jun-ichiro Ohe. Topological chiral magnonic edge mode in a magnonic crystal. *Physical Review B*, 87(17):174427, 2013.
- [18] Se Kwon Kim, Héctor Ochoa, Ricardo Zarzuela, and Yaroslav Tserkovnyak. Realization of the haldane-kane-mele model in a system of localized spins. *Physical Review Letters*, 117(22):227201, 2016.
- [19] Darshan G. Joshi. Topological excitations in the ferromagnetic kitaev-heisenberg model. *Phys. Rev. B*, 98:060405, Aug 2018.
- [20] Judit Romhányi, Karlo Penc, and Ramachandran Ganesh. Hall effect of triplons in a dimerized quantum magnet. *Nature communications*, 6(1):6805, 2015.
- [21] Darshan G Joshi and Andreas P Schnyder. Topological quantum paramagnet in a quantum spin ladder. *Physical Review B*, 96(22):220405, 2017.
- [22] Darshan G. Joshi and Andreas P. Schnyder. F_2 topological quantum paramagnet on a honeycomb bilayer. *Phys. Rev. B*, 100:020407, Jul 2019.
- [23] Andrii V Chumak, Vitaliy I Vasyuchka, Alexander A Serga, and Burkard Hillebrands. Magnon spintronics. *Nature physics*, 11(6):453–461, 2015.
- [24] Z-X Li, Yunshan Cao, and Peng Yan. Topological insulators and semimetals in classical magnetic systems. *Physics Reports*, 915:1–64, 2021.
- [25] Ryo Matsumoto and Shuichi Murakami. Theoretical prediction of a rotating magnon wave packet in ferromagnets. *Physical Review Letters*, 106(19):197202, 2011.
- [26] XS Wang, HW Zhang, and XR Wang. Topological magnonics: A paradigm for spin-wave manipulation and device design. *Physical Review Applied*, 9(2):024029, 2018.
- [27] Igor V Gornyi, Alexander D Mirlin, and Dmitry G Polyakov. Interacting electrons in disordered wires: Anderson localization and low-t transport. *Physical review letters*, 95(20):206603, 2005.
- [28] Rahul Nandkishore and David A Huse. Many-body localization and thermalization in quantum statistical mechanics. *Annu. Rev. Condens. Matter Phys.*, 6(1):15–38, 2015.
- [29] Ehud Altman and Ronen Vosk. Universal dynamics and renormalization in many-body-localized systems. *Annu. Rev. Condens. Matter Phys.*, 6(1):383–409, 2015.
- [30] Fabien Alet and Nicolas Laflorencie. Many-body localization: An introduction and selected topics. *Comptes Rendus Physique*, 19(6):498–525, 2018.
- [31] Dmitry A Abanin, Ehud Altman, Immanuel Bloch, and Maksym Serbyn. Colloquium: Many-body localization, thermalization, and entanglement. *Reviews of Modern Physics*, 91(2):021001, 2019.
- [32] Adam S Jermyn, Roger SK Mong, Jason Alicea, and Paul Fendley. Stability of zero modes in parafermion chains. *Physical Review B*, 90(16):165106, 2014.
- [33] Jack Kemp, Norman Y Yao, Christopher R Laumann, and Paul Fendley. Long coherence times for edge spins. *Journal of Statistical Mechanics: Theory and Experiment*, 2017(6):063105, 2017.
- [34] Dominic V Else, Paul Fendley, Jack Kemp, and Chetan Nayak. Prethermal strong zero modes and topological qubits. *Physical Review X*, 7(4):041062, 2017.
- [35] Maksym Serbyn, Dmitry A Abanin, and Zlatko Papić. Quantum many-body scars and weak breaking of ergodicity. *Nature Physics*, 17(6):675–685, 2021.
- [36] Anushya Chandran, Thomas Iadecola, Vedika Khemani, and Roderich Moessner. Quantum many-body scars: A quasiparticle perspective. *Annual Review of Condensed Matter Physics*, 14:443–469, 2023.
- [37] Sanjay Moudgalya, B Andrei Bernevig, and Nicolas Regnault. Quantum many-body scars and hilbert space fragmentation: a review of exact results. *Reports on Progress in Physics*, 85(8):086501, 2022.
- [38] Daniel E Parker, Romain Vasseur, and Thomas Scaffidi. Topologically protected long edge coherence times in symmetry-broken phases. *Physical Review Letters*, 122(24):240605, 2019.
- [39] Ivan Amelio and Iacopo Carusotto. Theory of the coherence of topological lasers. *Physical Review X*, 10(4):041060, 2020.
- [40] Petr Zapletal, Bogdan Galilo, and Andreas Nunnenkamp. Long-lived elementary excitations and light coherence in topological lasers. *Optica*, 7(9):1045–1055, 2020.
- [41] Yasaman Bahri, Ronen Vosk, Ehud Altman, and Ashvin Vishwanath. Localization and topology protected quantum coherence at the edge of hot matter. *Nature communications*, 6(1):7341, 2015.
- [42] Rajesh Chaunsali, Haitao Xu, Jinkyu Yang, Panayotis G Kevrekidis, and Georgios Theocharis. Stability of topological edge states under strong nonlinear effects. *Physical Review B*, 103(2):024106, 2021.
- [43] Daria Smirnova, Daniel Leykam, Yidong Chong, and Yuri Kivshar. Nonlinear topological photonics. *Applied Physics Reviews*, 7(2), 2020.
- [44] Daniel Leykam and Yi Dong Chong. Edge solitons in nonlinear-photonic topological insulators. *Physical review letters*, 117(14):143901, 2016.
- [45] Nathan Goldman, Jérôme Beugnon, and Fabrice Gerbier. Detecting chiral edge states in the hofstadter optical lattice. *Physical review letters*, 108(25):255303, 2012.
- [46] Nathan Goldman, Jean Dalibard, Alexandre Dauphin, Fabrice Gerbier, Maciej Lewenstein, Peter Zoller, and Ian B Spielman. Direct imaging of topological edge states in cold-atom systems. *Proceedings of the National Academy of Sciences*, 110(17):6736–6741, 2013.
- [47] Yuan Yao, Masahiro Sato, Tetsuya Nakamura, Nobuo Furukawa, and Masaki Oshikawa. Theory of electron spin resonance in one-dimensional topological insulators with spin-orbit couplings: Detection of edge states. *Physical Review B*, 96(20):205424, 2017.
- [48] António T Costa, Daniel Lourenço R Santos, Nuno MR Peres, and Joaquín Fernández-Rossier. Topological magnons in CrI_3 monolayers: an itinerant fermion description. *2D Materials*, 7(4):045031, 2020.
- [49] Shuyi Li and Andriy H Nevidomskyy. Topological weyl magnons and thermal hall effect in layered honeycomb

- ferromagnets. *Physical Review B*, 104(10):104419, 2021.
- [50] Kyusung Hwang, Nandini Trivedi, and Mohit Randeria. Topological magnons with nodal-line and triple-point degeneracies: implications for thermal hall effect in pyrochlore iridates. *Physical Review Letters*, 125(4):047203, 2020.
- [51] Pontus Laurell and Gregory A Fiete. Magnon thermal hall effect in kagome antiferromagnets with dzyaloshinskii-moriya interactions. *Physical Review B*, 98(9):094419, 2018.
- [52] Alexander Mook, Jürgen Henk, and Ingrid Mertig. Magnon hall effect and topology in kagome lattices: A theoretical investigation. *Physical Review B*, 89(13):134409, 2014.
- [53] SA Owerre. Topological honeycomb magnon hall effect: A calculation of thermal hall conductivity of magnetic spin excitations. *Journal of Applied Physics*, 120(4), 2016.
- [54] Jung Hoon Han and Hyunyoung Lee. Spin chirality and hall-like transport phenomena of spin excitations. *Journal of the Physical Society of Japan*, 86(1):011007, 2017.
- [55] Fengfeng Zhu, Lichuan Zhang, Xiao Wang, Flaviano José Dos Santos, Junda Song, Thomas Mueller, Karin Schmalzl, Wolfgang F Schmidt, Alexandre Ivanov, Jitae T Park, et al. Topological magnon insulators in two-dimensional van der waals ferromagnets crsite3 and crgete3: Toward intrinsic gap-tunability. *Science advances*, 7(37):eabi7532, 2021.
- [56] Heda Zhang, Chunqiang Xu, Caitlin Carnahan, Milos Sretenovic, Nishchay Suri, Di Xiao, and Xianglin Ke. Anomalous thermal hall effect in an insulating van der waals magnet. *Physical Review Letters*, 127(24):247202, 2021.
- [57] Paul A McClarty, F Krüger, Tatiana Guidi, SF Parker, Keith Refson, AW Parker, Dharmalingam Prabhakaran, and Radu Coldea. Topological triplon modes and bound states in a shastry–sutherland magnet. *Nature Physics*, 13(8):736–741, 2017.
- [58] Peter Czajka, Tong Gao, Max Hirschberger, Paula Lampen-Kelley, Arnab Banerjee, Nicholas Quirk, David G Mandrus, Stephen E Nagler, and N Phuan Ong. Planar thermal hall effect of topological bosons in the kitaev magnet α -rucl3. *Nature Materials*, 22(1):36–41, 2023.
- [59] Max Hirschberger, Robin Chisnell, Young S Lee, and Nai Phuan Ong. Thermal hall effect of spin excitations in a kagome magnet. *Physical Review Letters*, 115(10):106603, 2015.
- [60] Y Onose, T Ideue, H Katsura, Y Shiomi, N Nagaosa, and Y Tokura. Observation of the magnon hall effect. *Science*, 329(5989):297–299, 2010.
- [61] S Suetsugu, T Yokoi, K Totsuka, T Ono, I Tanaka, S Kasahara, Y Kasahara, Z Chengchao, H Kageyama, and Y Matsuda. Intrinsic suppression of the topological thermal hall effect in an exactly solvable quantum magnet. *Physical Review B*, 105(2):024415, 2022.
- [62] Luke Pritchard Cairns, J-Ph Reid, Robin Perry, Dharmalingam Prabhakaran, and Andrew Huxley. Thermal hall effect of topological triplons in srCu2 (bo3) 2. In *Proceedings of the International Conference on Strongly Correlated Electron Systems (SCES2019)*, page 011089, 2020.
- [63] ME Zhitomirsky and AL Chernyshev. Colloquium: Spontaneous magnon decays. *Reviews of Modern Physics*, 85(1):219, 2013.
- [64] Jonas Habel, Alexander Mook, Josef Willsher, and Johannes Knolle. Breakdown of chiral edge modes in topological magnon insulators. *arXiv preprint arXiv:2308.03168*, 2023.
- [65] Andreas Thomasen, Karlo Penc, Nic Shannon, and Judit Romhányi. Fragility of $z=2$ topological invariant characterizing triplet excitations in a bilayer kagome magnet. *Physical Review B*, 104(10):104412, 2021.
- [66] D Schmidiger, Pierre Bouillot, S Mühlbauer, S Gvasaliya, Corinna Kollath, Thierry Giamarchi, and A Zheludev. Spectral and thermodynamic properties of a strong-leg quantum spin ladder. *Physical review letters*, 108(16):167201, 2012.
- [67] Elbio Dagotto and TM Rice. Surprises on the way from one-to two-dimensional quantum magnets: The ladder materials. *Science*, 271(5249):618–623, 1996.
- [68] Subir Sachdev and RN Bhatt. Bond-operator representation of quantum spins: Mean-field theory of frustrated quantum heisenberg antiferromagnets. *Physical Review B*, 41(13):9323, 1990.
- [69] Darshan G. Joshi, Kris Coester, Kai P. Schmidt, and Matthias Vojta. Nonlinear bond-operator theory and $1/d$ expansion for coupled-dimer magnets. i. paramagnetic phase. *Phys. Rev. B*, 91:094404, Mar 2015.
- [70] Darshan G. Joshi and Matthias Vojta. Nonlinear bond-operator theory and $1/d$ expansion for coupled-dimer magnets. ii. antiferromagnetic phase and quantum phase transition. *Phys. Rev. B*, 91:094405, Mar 2015.
- [71] Song Bao, Jinghui Wang, Wei Wang, Zhengwei Cai, Shichao Li, Zhen Ma, Di Wang, Kejing Ran, Zhao-Yang Dong, DL Abernathy, et al. Discovery of coexisting dirac and triply degenerate magnons in a three-dimensional antiferromagnet. *Nature communications*, 9(1):2591, 2018.
- [72] M Elliot, Paul A McClarty, D Prabhakaran, RD Johnson, HC Walker, P Manuel, and R Coldea. Order-by-disorder from bond-dependent exchange and intensity signature of nodal quasiparticles in a honeycomb cobaltate. *Nature Communications*, 12(1):3936, 2021.
- [73] Weiliang Yao, Chenyuan Li, Lichen Wang, Shangjie Xue, Yang Dan, Kazuki Iida, Kazuya Kamazawa, Kangkang Li, Chen Fang, and Yuan Li. Topological spin excitations in a three-dimensional antiferromagnet. *Nature Physics*, 14(10):1011–1015, 2018.
- [74] Bo Yuan, Iliia Khait, Guo-Jiun Shu, FC Chou, MB Stone, JP Clancy, Arun Paramakanti, and Young-June Kim. Dirac magnons in a honeycomb lattice quantum xy magnet cotio 3. *Physical Review X*, 10(1):011062, 2020.
- [75] L-C Zhang, YA Onykienko, PM Buhl, YV Tymoshenko, P Čermák, A Schneidewind, JR Stewart, A Henschel, M Schmidt, S Blügel, et al. Magnonic weyl states in cu 2 oseo 3. *Physical review research*, 2(1):013063, 2020.
- [76] Olivier Mentré, El Mostafa Ketatni, Marie Colmont, Marielle Huve, Francis Abraham, and Vaclav Petricek. Structural features of the modulated bicu2 (p1-x v x) o6 solid solution; 4-d treatment of x= 0.87 compound and magnetic spin-gap to gapless transition in new cu2+ two-leg ladder systems. *Journal of the American Chemical Society*, 128(33):10857–10867, 2006.

- [77] Frédéric Mila, Patrice Millet, and Jacques Bonvoisin. Exchange integrals of vanadates as revealed by magnetic-susceptibility measurements of NaV_2O_5 . *Physical Review B*, 54(17):11925, 1996.
- [78] Masahiko Isobe and Yutaka Ueda. Magnetic susceptibility of quasi-one-dimensional compound $\alpha\text{-NaVO}_2$ —possible spin-Peierls compound with high critical temperature of 34 K. *Journal of the Physical Society of Japan*, 65(5):1178–1181, 1996.
- [79] Z Hiroi and M Takano. Absence of superconductivity in the doped antiferromagnetic spin-ladder compound $(\text{La}, \text{Sr})\text{CuO}_2$. *Nature*, 377(6544):41–43, 1995.
- [80] Yoshimitsu Kohama, Shuang Wang, Atsuko Uchida, Krunoslav Prsa, Sergei Zvyagin, Yuri Skourski, Ross D McDonald, Luis Balicas, Henrik M Ronnow, Christian Rüegg, et al. Anisotropic cascade of field-induced phase transitions in the frustrated spin-ladder system BiCu_2PO_6 . *Physical Review Letters*, 109(16):167204, 2012.
- [81] V Kiryukhin, YJ Kim, KJ Thomas, FC Chou, RW Erwin, Q Huang, MA Kastner, and RJ Birgeneau. Magnetic properties of the $s=1/2$ quasi-one-dimensional antiferromagnet CaCu_2O_3 . *Physical Review B*, 63(14):144418, 2001.
- [82] Masaki Azuma, Z Hiroi, M Takano, K Ishida, and Y Kitaoka. Observation of a spin gap in SrCu_2O_3 comprising spin-1/2 quasi-1d two-leg ladders. *Physical Review Letters*, 73(25):3463, 1994.
- [83] Ya-ping Wang, Chang-wen Zhang, Wei-xiao Ji, Runwu Zhang, Ping Li, Pei-ji Wang, Miao-juan Ren, Xinlian Chen, and Min Yuan. Tunable quantum spin hall effect via strain in two-dimensional arsenene monolayer. *Journal of Physics D: Applied Physics*, 49(5):055305, 2016.
- [84] Chi-Ho Cheung, Huei-Ru Fuh, Ming-Chien Hsu, Yeu-Chung Lin, and Ching-Ray Chang. Spin orbit coupling gap and indirect gap in strain-tuned topological insulator-antimonene. *Nanoscale Research Letters*, 11:1–8, 2016.
- [85] Lars Winterfeld, Luis A Agapito, Jin Li, Nicholas Kioussis, Peter Blaha, and Yong P Chen. Strain-induced topological insulator phase transition in HgSe . *Physical Review B*, 87(7):075143, 2013.
- [86] Tsai-Jung Liu, Maximilian A Springer, Niclas Heinsdorf, Agnieszka Kuc, Roser Valentí, and Thomas Heine. Semimetallic square-octagon two-dimensional polymer with high mobility. *Physical Review B*, 104(20):205419, 2021.
- [87] K. Sturm. Dynamic structure factor: An introduction. *Zeitschrift für Naturforschung A*, 48(1-2):233–242, 1993.
- [88] Léon Van Hove. Correlations in space and time and Born approximation scattering in systems of interacting particles. *Physical Review*, 95(1):249, 1954.
- [89] Darshan G Joshi, Andreas P Schnyder, and So Takei. Detecting end states of topological quantum paramagnets via spin hall noise spectroscopy. *Physical Review B*, 98(6):064401, 2018.
- [90] Steven R White. Density matrix formulation for quantum renormalization groups. *Physical Review Letters*, 69(19):2863, 1992.
- [91] Guifré Vidal. Efficient simulation of one-dimensional quantum many-body systems. *Physical Review Letters*, 93(4):040502, 2004.
- [92] Andrew John Daley, Corinna Kollath, Ulrich Schollwöck, and Guifré Vidal. Time-dependent density-matrix renormalization-group using adaptive effective Hilbert spaces. *Journal of Statistical Mechanics: Theory and Experiment*, 2004(04):P04005, 2004.
- [93] Steven R White and Adrian E Feiguin. Real-time evolution using the density matrix renormalization group. *Physical Review Letters*, 93(7):076401, 2004.
- [94] Jutho Haegeman, J Ignacio Cirac, Tobias J Osborne, Iztok Pizorn, Henri Verschelde, and Frank Verstraete. Time-dependent variational principle for quantum lattices. *Physical Review Letters*, 107(7):070601, 2011.
- [95] Jutho Haegeman, Christian Lubich, Ivan Oseledets, Bart Vandereycken, and Frank Verstraete. Unifying time evolution and optimization with matrix product states. *Physical Review B*, 94(16):165116, 2016.
- [96] Michael P Zaletel, Roger SK Mong, Christoph Karrasch, Joel E Moore, and Frank Pollmann. Time-evolving a matrix product state with long-ranged interactions. *Physical Review B*, 91(16):165112, 2015.
- [97] Nicholas E Sherman, Maxime Dupont, and Joel E Moore. Spectral function of the j_1-j_2 Heisenberg model on the triangular lattice. *Physical Review B*, 107(16):165146, 2023.
- [98] Pierre Bouillot, Corinna Kollath, Andreas M Läuchli, Mikhail Zvonarev, Benedikt Thielemann, Christian Rüegg, Edmond Orignac, Roberta Citro, Martin Klanjšek, Claude Berthier, et al. Statics and dynamics of weakly coupled antiferromagnetic spin-1 ladders in a magnetic field. *Physical Review B*, 83(5):054407, 2011.
- [99] Pontus Laurell, Allen Scheie, D Alan Tennant, Satoshi Okamoto, Gonzalo Alvarez, and Elbio Dagotto. Magnetic excitations, nonclassicality, and quantum wake spin dynamics in the Hubbard chain. *Physical Review B*, 106(8):085110, 2022.
- [100] Matthias Gohlke, Roderich Moessner, and Frank Pollmann. Dynamical and topological properties of the Kitaev model in a [111] magnetic field. *Physical Review B*, 98(1):014418, 2018.
- [101] supplemental.
- [102] Rhine Samajdar, Mathias S Scheurer, Shubhayu Chatterjee, Haoyu Guo, Cenke Xu, and Subir Sachdev. Enhanced thermal Hall effect in the square-lattice Néel state. *Nature Physics*, 15(12):1290–1294, 2019.
- [103] Masataka Kawano and Chisa Hotta. Thermal Hall effect and topological edge states in a square-lattice antiferromagnet. *Physical Review B*, 99(5):054422, 2019.
- [104] Xiaodong Cao, Kai Chen, and Dahai He. Magnon Hall effect on the Lieb lattice. *Journal of Physics: Condensed Matter*, 27(16):166003, 2015.
- [105] B Sriram Shastry and Bill Sutherland. Exact ground state of a quantum mechanical antiferromagnet. *Physica B+C*, 108(1-3):1069–1070, 1981.
- [106] Chunyu Guo, Lunhui Hu, Carsten Putzke, Jonas Diaz, Xiangwei Huang, Kaustuv Manna, Feng-Ren Fan, Chandra Shekhar, Yan Sun, Claudia Felser, et al. Quasi-symmetry-protected topology in a semi-metal. *Nature Physics*, 18(7):813–818, 2022.
- [107] Chao Shang, Owen Ganter, Niclas Heinsdorf, and Stephen M Winter. Ir_4 : From tetrahedral compass model to topological semimetal. *Physical Review B*, 107(12):125111, 2023.
- [108] Victor Gurarie. Single-particle Green's functions and interacting topological insulators. *Physical Review B*,

- 83(8):085426, 2011.
- [109] Zhong Wang and Binghai Yan. Topological hamiltonian as an exact tool for topological invariants. *Journal of Physics: Condensed Matter*, 25(15):155601, 2013.
- [110] Zhong Wang and Shou-Cheng Zhang. Simplified topological invariants for interacting insulators. *Physical Review X*, 2(3):031008, 2012.
- [111] Mikel Iraola, Niclas Heinsdorf, Apoorv Tiwari, Dominik Lessnich, Thomas Mertz, Francesco Ferrari, Mark H Fischer, Stephen M Winter, Frank Pollmann, Titus Neupert, et al. Towards a topological quantum chemistry description of correlated systems: The case of the hubbard diamond chain. *Physical Review B*, 104(19):195125, 2021.
- [112] Anton Kapustin and Lev Spodyneiko. Higher-dimensional generalizations of berry curvature. *Physical Review B*, 101(23):235130, 2020.
- [113] Ken Shiozaki, Niclas Heinsdorf, and Shuhei Ohyama. Higher berry curvature from matrix product states. *arXiv preprint arXiv:2305.08109*, 2023.
- [114] Philipp Hauke, Markus Heyl, Luca Tagliacozzo, and Peter Zoller. Measuring multipartite entanglement through dynamic susceptibilities. *Nature Physics*, 12(8):778–782, 2016.
- [115] Johannes Hauschild and Frank Pollmann. Efficient numerical simulations with tensor networks: Tensor network python (tenpy). *SciPost Physics Lecture Notes*, page 005, 2018.
- [116] Charles R. Harris, K. Jarrod Millman, Stéfan J. van der Walt, Ralf Gommers, Pauli Virtanen, David Cournapeau, Eric Wieser, Julian Taylor, Sebastian Berg, Nathaniel J. Smith, Robert Kern, Matti Picus, Stephan Hoyer, Marten H. van Kerkwijk, Matthew Brett, Allan Haldane, Jaime Fernández del Río, Mark Wiebe, Pearu Peterson, Pierre Gérard-Marchant, Kevin Sheppard, Tyler Reddy, Warren Weckesser, Hameer Abbasi, Christoph Gohlke, and Travis E. Oliphant. Array programming with NumPy. *Nature*, 585(7825):357–362, September 2020.
- [117] Niclas Heinsdorf. topwave python package. to be published, see Supplementary.

SUPPLEMENTARY MATERIAL

I. DMRG AND TIME-EVOLUTION

We use DMRG and the \hat{W}^{II} time-evolution method as implemented in the tenpy package [115]. The sampling rate (or time step Δt) is chosen such that the fastest frequency of the signal is resolved, which is the ground state frequency ω_0 . The resolution of the Fourier transformed output along the frequency axis - but also the severity of finite size effects due to reflections at the boundaries - is then determined by the total evolved time $T = N_{\Delta t} \Delta t$, where $N_{\Delta t}$ is the number of time steps.

To reduce ringing effects the correlation functions are convoluted with a hamming window along the time axis, before being Fourier transformed using Fast Fourier Transform (FFT) as implemented in the numpy package [116]. To obtain the Fourier transform in real-space,

all matrix elements C_{ij} are collected with respect to their relative distance along the ladder $d = i - j$.

Because the DSF is a response function, it is required to be real and positive. In principle, this can be used to choose a suitable Fourier transform, the output of which will always meet said requirements. In this work, we choose an agnostic, pre-implemented FFT to be able to judge the severity of finite-size and -time effects by keeping track of the deviations from these properties as well as the violation of sum rules.

The algorithm that is used to compute the DSF is summarized as follows:

1. Compute ground state $|\psi_0\rangle$ using (finite) DMRG.
2. Compute $|\psi_j^{\gamma'}(t=0)\rangle = \hat{S}_j^{\gamma'} |\psi_0\rangle$.
3. Time-evolve one time step using \hat{W}^{II} :

$$\hat{U}(\Delta t) |\psi_j^{\gamma'}(t=0)\rangle = |\psi_j^{\gamma'}(t+\Delta t)\rangle$$
4. Compute $|\psi_{ij}^{\gamma\gamma'}(t+\Delta t)\rangle = \hat{S}_j^{\gamma'} |\psi_i^{\gamma}(t+\Delta t)\rangle$ for all i .
5. Compute overlap $C_{ij}^{\gamma\gamma'}(t+\Delta t) = \langle \psi_0 | \psi_{ij}^{\gamma\gamma'}(t+\Delta t) \rangle$
6. Repeat steps 3 - 5 $N_{\Delta t} = T/\Delta t$ times.
7. Repeat steps 2 - 6 for all j .
8. Fourier transform $C_{ij}^{\gamma\gamma'}(t)$ in time and sites.

II. CASE (I): STRONG FIELD AND LINEAR SPIN WAVE THEORY

For strong external magnetic fields $h_y/J \sim 1$, there is a transition to the field polarized phase as can be seen in Fig. S1. This ordered state has magnons as its low-lying excitations. We perform Linear Spin Wave Theory (LSWT) as implemented in the topwave package[117], and plot the magnon band structures for a variety of different parameters in Fig. S2. In the parameter regime relevant to our model, no band crossing can be enforced.

III. CASE (II): STRONG RAIL COUPLING

In the limit of strong rail coupling K , the ladder model resembles two weakly coupled anti-ferromagnetic Heisenberg chains. We define the antiferromagnetic order parameter (for the left rail) as

$$\Delta^{\text{AFM}} = \frac{1}{(L/2)^2} \sum_{\gamma=x,y,z} \sum_{i,j}^L (-1)^{i+j} \langle \hat{S}_i^{\gamma} \hat{S}_j^{\gamma} \rangle / 3. \quad (12)$$

The order parameter for the right rail ($\alpha = r$) is equivalent. For finite system size and finite SOC, the order parameter is nonzero, but approaches zero for larger system sizes as shown in Fig. S3. Hence, the system does not order, as expected for one dimension.

IV. CASE (III): STRONG SPIN-ORBIT COUPLING

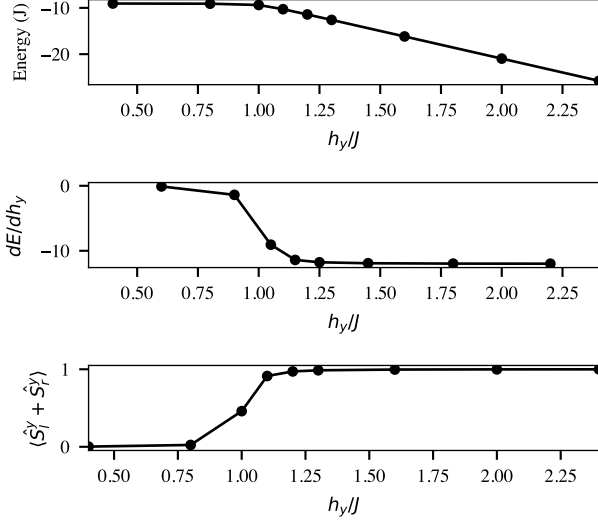


FIG. S1. The ground state energy, its derivative and the magnetization along the external field axis as a function of field strength h_y/J . At $h_y/J \sim 1$ there is a phase transition from the paramagnetic to the field-polarized phase.

Even though SOC gaps out the two triplon modes, the lower mode does not condense even for large values of D_y and Γ_y . In Fig. S4 the ground state energy and its derivatives are given. There is no sign of a phase transition. Fig. S5 shows the logarithm of the DSF for strong SOC ($\Gamma_y = D_y = 2.6J$) and no magnetic field. The two triplon modes are split into many different energy levels, which are completely flat. The lower modes do not condense, but are instead “repelled” while the upper modes rise in energy and are strongly damped. The topological boundary mode is stable.

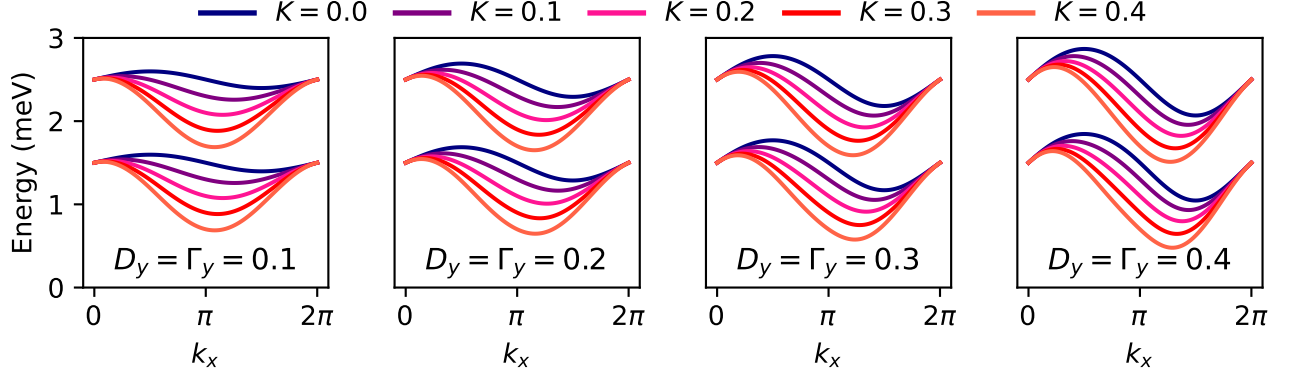


FIG. S2. Magnon spectra of the field polarized ladder for $h_y/J = 2.5$ obtained by LSWT as implemented in the topwave package[117] for different values of rail coupling K and SOC. The model has two magnetic sites per unit cell and hence two magnon bands. Two bands of the same model are given in the same color. There are no band crossings and the bands are topologically trivial.

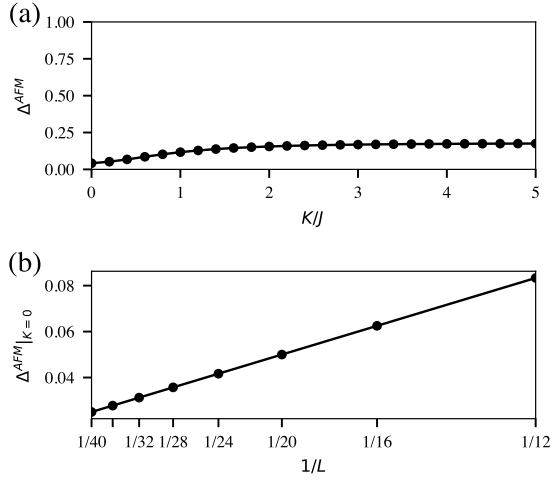


FIG. S3. (a) Antiferromagnetic order parameter for $h_y = 0$, $D_y = \Gamma_y = 0.1J$ on a ladder with $L = 24$ rungs. The order parameter is small, but finite even for $K = 0$. (b) Finite size scaling of the order parameter at $K = 0$. The order parameter approaches zero in the thermodynamic limit.

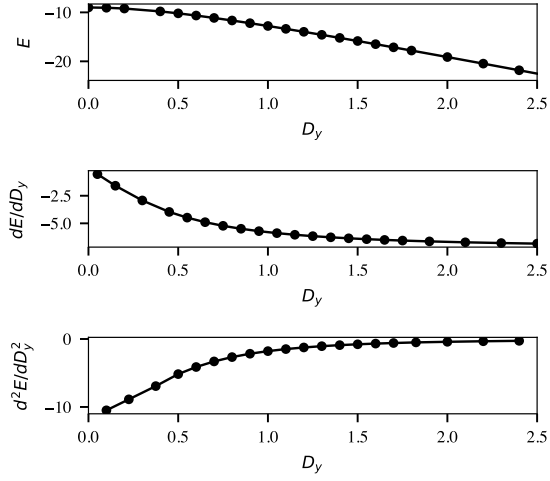


FIG. S4. Ground state energy (a) and its first (b) and second (c) derivative with respect to SOC D_y (in units of J) with $K = 0.01J$, $h_y = 0$ and $\Gamma_y = D_y$ on a ladder with $L = 12$ rungs. The curves are smooth and there is no evidence of a phase transition.

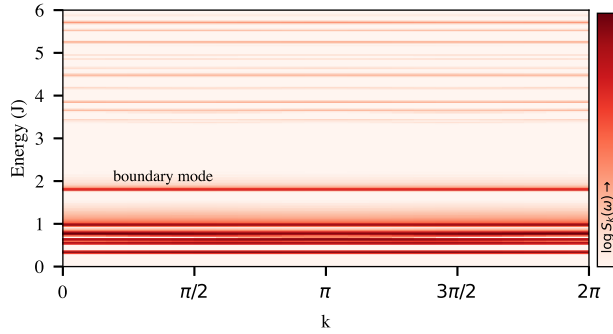


FIG. S5. The logarithm of the DSF for $K = 0.01J$, $h_y = 0$ and $\Gamma_y = D_y = 2.6J$ on a ladder with $L = 12$ rungs. There are many flat energy levels with the ones at higher energies being damped strongly. The boundary mode remains present and is marked.